Available online at www.sciencedirect.com
SCIENCE DIRECT®
Physica B 348 (2004) 397–403
PHYSICA B
www.elsevier.com/locate/physb

Experimental determination of the laterally homogeneous barrier height of Au/*n*-Si Schottky barrier diodes

M. Sağlam, F.E. Cimilli, A. Türüt*

Faculty of Sciences and Arts, Department of Physics, Atatürk University, Erzurum 25240, Turkey

Received 3 November 2003; received in revised form 17 December 2003; accepted 2 January 2004

Abstract

We have computed the homogeneous barrier height (BH) of Au/*n*-Si Schottky diodes (SDs). Thereby, Au/*n*-Si/Au–Sb SDs (24 dots) have identically been prepared, and the effective BHs and ideality factors of these diodes have been calculated from their experimental forward bias current–voltage ($I-V$) and reverse bias capacitance–voltage ($C-V$) characteristics. The BH for the Au/*n*-Si/Au–Sb diodes from the $I-V$ characteristics varied from 0.789 to 0.819 eV, the ideality factor n varied from 1.051 to 1.179, and the BH from $C^{-2}-V$ characteristics varied from 0.801 to 0.851 eV. The Gaussian fits of he experimental Schottky BH distributions obtained from the $C^{-2}-V$ and $I-V$ characteristics have yielded a mean BH values of 0.808 and 0.809 eV, respectively, that are in close agreement with value of about 0.805 eV predicted by metal-induced gap states (MIGS) and chemical electronegativity concepts for Au/*n*-Si SDs. Furthermore, the lateral homogeneous BH value of approximately 0.834 eV were also computed from the extrapolation of the linear plot of experimental BHs versus ideality factors.
© 2004 Elsevier B.V. All rights reserved.

Keywords: Metal–semiconductor contact; Schottky barrier; Barrier inhomogeneity

1. Introduction

The physical properties of metal–semiconductor interfaces are widely studied, both for their basic physical properties and for their technological applications to electronic devices. Although Schottky interfaces have been well studied for over 50 years, it is only in the past decade that an inhomogeneous contact [1–7] has been considered as an explanation for a voltage-dependent barrier height (BH). In real structures, the variation of BH may arise from differences in interface layer thickness, composition or inhomogeneties in the distribution of interface charge [2,8]. Ohdomari and Tu [9] discussed a contact formed by two phases with a high and low barrier. They found that such a structure behaves like a diode with an apparent single BH. The apparent BH is a function of the local BHs Φ_L and Φ_H and pertaining areas S_L and S_H. Because of the exponential dependence of the current on BH, the majority of the current will flow through the lower barrier part of the contact. The existence of small local regions (patches) with a different BH was evidenced experimentally by using ballistic electron emission

*Corresponding author. Tel.: +90-442-231-4171; fax: +90-442-236-0948.
E-mail address: aturut@atauni.edu.tr (A. Türüt).

0921-4526/$ - see front matter © 2004 Elsevier B.V. All rights reserved.
doi:10.1016/j.physb.2004.01.002

spectroscopy (BEES) [10–12]. As mentioned in Refs. [3–5,13], the BH is likely to be a function of the interface atomic structure, and the atomic inhomogeneities at the metal–semiconductor interface which are caused by grain boundaries, multiple phases, facets, defects, a mixture of different phases, etc. Song et al. [2] have also suggested that the barrier inhomogeneities can occur as a result of inhomogeneities in the interfacial oxide layer composition, nonuniformity of the interfacial charges and interfacial oxide layer thickness.

The experimental effective BHs and ideality factors obtained from the current–voltage $(I-V)$ and capacitance–voltage $(C-V)$ characteristics differ from diode to diode even if they are identically prepared [3,13–18]. That is, the BHs become smaller as the ideality factors increase. This finding has been attributed to patchy interfaces, i.e., to lateral inhomogeneities of the BH [4,13]. Tung [4] says that these results are hard to explain with interface gap states because the gap states are usually assumed to have implications for the magnitude of the BH and ideality factor of a Schottky barrier diode.

It is well known that, in a metal–semiconductor system, the Fermi level within the semiconductor band gap determines the formation of the BH. In general, the exact position of Fermi level depends on the details of the interface [2,16,19]. The BH of metal–semiconductor contacts is almost independent on the metal work function. Such a behavior indicates that some mechanisms must be responsible for the Fermi level pinning, such as metal-induced gap states (MIGS) [3,5,13,15,20] and defect models [15,16,20]. In the ideal Schottky diodes (SDs) (defect free interface), charge-neutrality level (CNL) of the MIGS may be considered to be the physical mechanism, which determines the BHs [15,16,20,21]. These states originate from the tails of the metal wave functions into the semiconductor. Our purpose in the present study is to compute the laterally homogeneous BH of Au/*n*-Si SDs (24 dots) that are prepared on the *n*-Si semiconductor. The effective BHs and ideality factors from the experimental forward bias current–voltage and reverse bias capacitance–voltage of these diodes have been calculated.

2. Experimental procedure

The samples have been prepared using cleaned and polished *n*-type Si wafer with [1 0 0] orientation and 2–5 Ω cm resistivity and 300 μm thickness. Before making contacts, the wafer was chemically cleaned using the RCA cleaning procedure (i.e. a 10 min boil in $NH_3+H_2O_2+6H_2O$ followed by a 10 min boil in $HCl+H_2O_2+6H_2O$) with the final dip in diluted HF for 30 s, and then rinsed in DI water with ultrasonic vibration and dried by high-purity nitrogen. The ohmic contact on the back surface of the wafer was made by evaporating Au–Sb alloy, followed by a temperature treatment at 420°C for 3 min in N_2 atmosphere. The native oxide on the front surface of the substrate was removed in HF:H_2O (1:10) solution and finally the wafer was rinsed in de-ionized water for 30 s. Then, the Schottky contacts were formed by evaporation of Au dots with diameter of about 1.0 mm (the diode area $=7.85\times10^{-3}\,\mathrm{cm}^2$). The current–voltage and capacitance–voltage characteristics were measured using a HP 4140B picoammeter and a HP model 4192A LF impedance analyser, respectively, at room temperature and in the dark.

3. Results and discussion

The diode parameters are determined from the forward bias current–voltage $(I-V)$ characteristics, which is usually described within the thermionic emission theory [19,22,23]

$$I = I_0\left[\exp\left(\frac{qV}{nkT}\right)-1\right], \tag{1}$$

where the saturation current I_0 is expressed as

$$I_0 = AA^*T^2\exp\left(\frac{-q\Phi_b}{kT}\right), \tag{2}$$

where q is the electron charge, V the applied voltage, A^* the effective Richardson constant and equals to $112\,\mathrm{A\,cm^{-2}\,K^2}$ for *n*-type Si [19], A the effective diode area, T the absolute temperature, k the Boltzmann constant, n the ideality factor of a Schottky barrier diode, and Φ_b is the zero bias BH. For values of V greater than $3kT/q$, the ideality

factor from Eq. (1) can be written as

$$n = \frac{q}{kT}\frac{\Delta V}{\Delta \ln I}. \quad (3)$$

The experimental semi-log-forward bias characteristics of the Au/*n*-Si/Au–Sb SDs are shown in Fig. 1. We fabricated 24 dots (Schottky contacts) for the Au/*n*-Si(1 0 0) Schottky barrier diodes on the same *n*-type semiconductor substrate. The Schottky BH ϕ_b for the diodes ranged from 0.819 to 0.789 eV, and ideality factor n varied from 1.051 to 1.179.

In SDs, the depletion layer capacitance, C can be expressed as [22]:

$$C^{-2} = 2(V_0 + V)/q\varepsilon_s A^2 N_D, \quad (4)$$

where A is the area of the diode, V_0 is the diffusion potential at zero bias and is determined from the extrapolation of the linear $C^{-2}-V$ plot to the V axis, ε_s is the dielectric constant of the semiconductor, N_D is the donor concentration of *n*-type semiconductor substrate. The plots of C^{-2} as a function of reverse bias voltage are linear that indicates the formation of SDs [24]. With the help of Eq. (4), the values of V_0 and N_D can be determined from the intercept and slope of the $C^{-2}-V$ plot. Fig. 2 shows the room temperature reverse bias $C^{-2}-V$ characteristics of the Au/*n*-Si SDs (24 dots) at 1.0 MHz. The capacitance–voltage BH for the Au/*n*-Si diodes ranged from 0.801 to 0.851 eV.

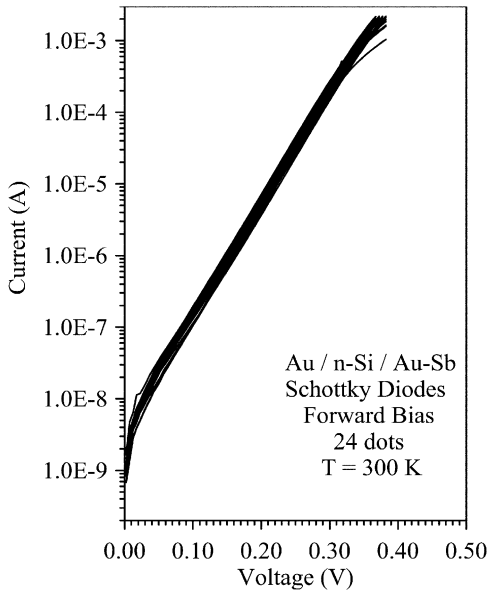


Fig. 1. Experimental semi-log-forward bias characteristics of the Au/*n*-Si SDs at room temperature.

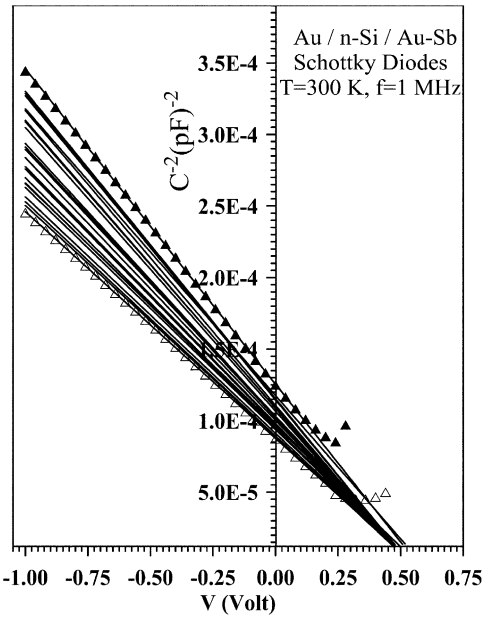


Fig. 2. Reverse bias $C^{-2}-V$ characteristics of the Au/*n*-Si SDs at a frequency of 1.0 MHz and room temperature.

As can be seen, the effective Schottky BH from $I-V$ and $C-V$ characteristics varied from diode to diode. Therefore, it is common practice to take averages [11–18,25,26]. Fig. 3 shows the statistical distribution of BHs from the forward bias $I-V$ plots of the Au/*n*-Si Schottky barrier diodes (24 dots) and Fig. 4 shows the statistical distribution of BHs from the reverse bias $C^{-2}-V$ plots of the same diodes. The experimental distributions of the effective BHs were fitted by the Gaussian function. At first, let us consider the $I-V$ BHs. The statistical analysis yielded a mean BH value of 0.809 eV with a standard deviation of 5.28 meV. In the distribution of the BHs from the reverse bias $C^{-2}-V$ characteristics of the Au/*n*-Si SDs at 1.0 MHz (Fig. 4), the Gaussian fit yields a mean BH value of 0.808 eV with standard deviation of 5.18 meV. As can be seen, the mean values of Φ_b obtained from $I-V$ and $C^{-2}-V$ characteristics are approximately equal to each other. In the

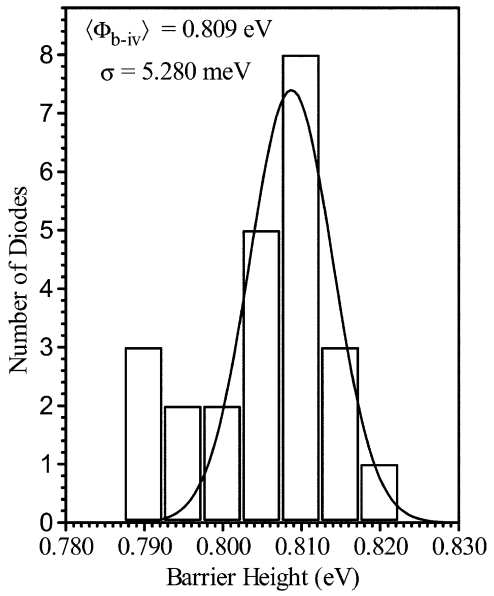


Fig. 3. Distribution of BHs from the forward bias $I-V$ characteristics of the diodes at room temperature.

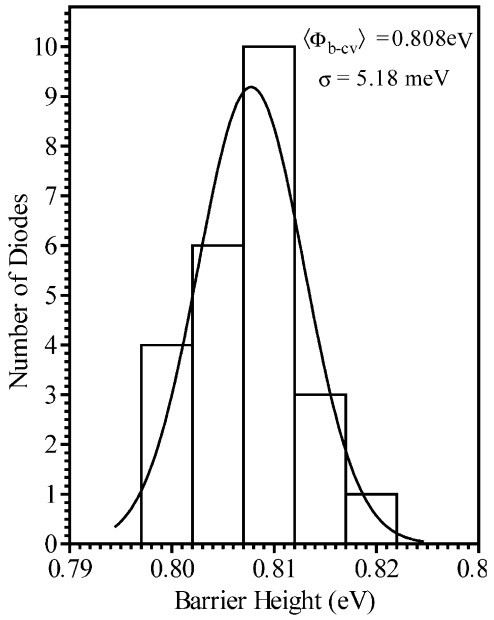


Fig. 4. Distribution of BHs from the reverse bias $C^{-2}-V$ characteristics of the diodes at 1.0 MHz and room temperature.

distribution of the ideality factors from the forward bias $I-V$ characteristics of the Au/*n*-Si SDs (Fig. 5), the Gaussian fit yields a mean ideality

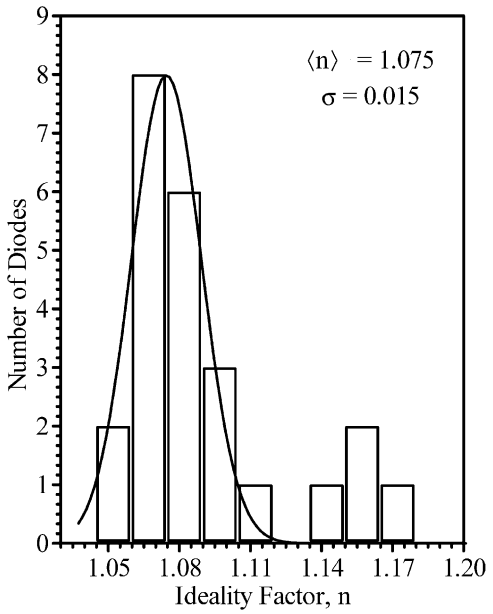


Fig. 5. Distribution of ideality factors from the forward bias $I-V$ characteristics of the diodes at room temperature.

factor value of 1.075 with a standard deviation of 0.015. Fig. 6 shows the statistical distribution of carrier concentrations from the reverse bias $C^{-2}-V$ characteristics of the Au/*n*-Si SDs and the Gaussian distribution of carrier concentrations of the diodes has yielded $N_D = 1.04 \times 10^{15}\,cm^{-3}$ with $\sigma = 1.38 \times 10^{14}\,cm^{-3}$.

Fig. 7 shows a plot of the experimental BHs versus the ideality factors at room temperature. As can be seen from Fig. 7, there is a linear relationship between experimental effective BHs and ideality factors of the Schottky contacts that has been explained by lateral inhomogeneities of the BHs in SDs [3–7,15–18]. That is, the BHs become smaller as the ideality factors increase. This finding may be attributed to lateral inhomogeneities of the BHs in SDs [2–6,14–18]. In addition, Tung [4] and Mönch and co-workers [15–18] have found that, among identically prepared diodes, higher ideality factors have accompanied lower observed BHs. This inhomogeneity model is based on small local regions or patches. The ideality factor that is determined by the image-force effect only should be close to 1.01 or 1.02 [2,4–6,19,22]. Our data clearly show that the diodes have ideality factors

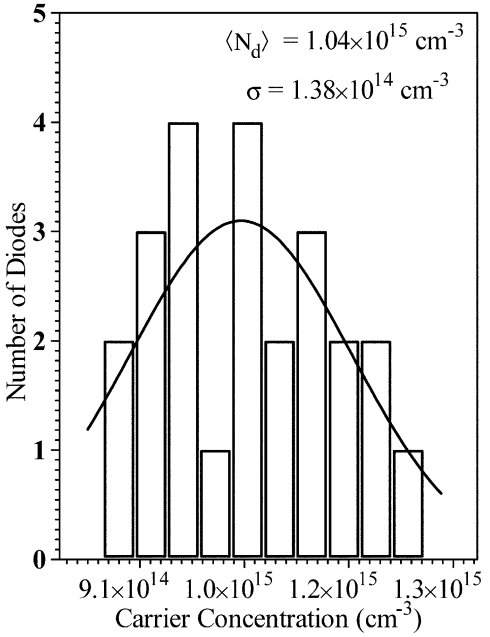


Fig. 6. Distribution of carrier concentrations from the reverse bias $C^{-2}-V$ characteristics of the diodes at 1.0 MHz and room temperature.

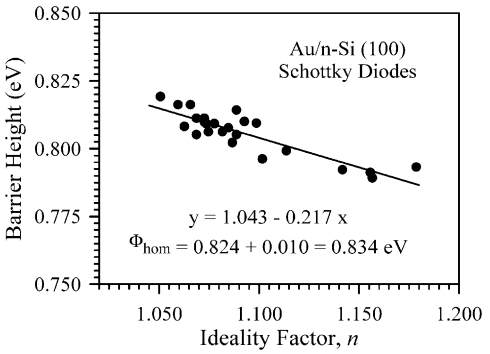


Fig. 7. Plot of experimental BH versus ideality factor of the Au/*n*-Si SDs at room temperature.

that are considerably larger than the value determined by the image-force effect only. Therefore, these diodes are patchy [15–18]. The straight line in Fig. 7 is a least squares fit to the experimental data. The extrapolation of the plot to $n_{if} = 1.01$, determined by the image-force effect, results in the laterally homogeneous BHs of approximately 0.834 eV for the Au/*n*-Si Schottky barrier diodes, adding the image force lowering values. Thus, there is a difference of 0.026 eV between the mean effective BH [$\Phi_b(C-V) = 0.808$ eV] and homogeneous BH for the Au/*n*-Si diodes. This small discrepancy is obviously caused by the small ideality factor of the Au/*n*-Si diodes. The image-force lowering value for the ideality factor n_{if} was determined by using Eq. (19.14) in Ref. [17].

It has been proposed that the fabrication-induced interface defects could exist in addition to metal-induced gap states (MIGS) and alter the BH [17]. The defects give rise to additional discrete levels in the band gap and the Fermi level is pinned to one of these levels, possibly quite far away from the charge neutrality level (CNL). Again, the formation of the BHs may be attributed to their chemical trends, i.e. to the differences in electronegativity between semiconductor and metal. In generalizing the above concept, the charge transfer at metal–semiconductor contacts will be characterized by the electronegativity difference of the metal and semiconductor in the contact [17,21]. Again, it has been attributed in Refs. [17,18] that the formation of the BHs to their chemical trends, i.e., to the differences in electronegativity between semiconductor and metal. In generalizing, the transfer of charges at metal–semiconductor contacts will be characterized by the electronegativity difference of the metal and semiconductor in the contact. The MIGS line in the laterally homogeneous BHs versus electronegativity difference plot for *n*-Si (Fig. 6 in Ref. [18]) gives the following relation:

$$\Phi_{bn} = 0.760 + 0.101(X_m - X_s), \quad (5)$$

where X_m and X_s are the electronegativities of the metal and semiconductor, respectively, and the value of 0.760 eV is the zero-charge-transfer BHs of the MIGS with respect to the bottom of the conduction band at the surface of the semiconductor. The electronegativity values for the metal Au and semiconductor Si were taken as $X_m = 5.15$ eV and $X_s = 4.70$ [17], respectively. This expression gives the BH value of about 0.805 eV for Au/*n*-Si SDs. Thus, the laterally homogeneous BHs of approximately 0.834 eV (Fig. 7) for the Au/*n*-Si contacts is close to the MIGS line of

n-Si/metal contacts for the value of 0.029 eV. The slight difference in the Schottky BH of the laterally homogeneous contacts may be easily attributed to the margins of error in the analysis of the experimental $I-V$ characteristics. Eq. (5) gives the BH value of about 0.805 eV for Au/n-Si contact that is in close agreement with the mean value of $\bar{\Phi}_b(C-V) = 0.808$ eV from the $C^{-2}-V$ characteristic.

As indicated above, BEEM studies on real Schottky contacts demonstrates the existence of lateral variations of their BHs on the nanometer scale and the existence of the patches with a different BH, that is, the contacts posses the lateral inhomogeneities on the nanometer scale [4,13,27,28]. As mentioned in Refs. [4,13,27], as the low-BH radius decreases, the patches become more pinched-off (i.e., if the patch radius is much less than the depletion region width, the potential at the saddle point increases). At some critical patch size, there is no pinch-off, for patches much larger than the critical size, the potential distribution approaches that of a uniform MS contact. Likely, when the BH difference is less than critical value, there is no potential pinch-off, and for larger BH difference is, the degree of the pinch-off increases. As the BH difference approaches zero, the potential profiles approaches those of a MS contact with uniform BH. Again, the BH at high temperature appears more uniform than that at low temperature.

The model of potential fluctuations in Refs. [2,6,7,28] allows for an analytical description of the temperature dependent transport properties of Schottky contacts with a continuous range of spatially distributed barriers. The model considers fluctuations of band bending and Schottky barriers that occur on a length scale small compared to the width of the space-charge region. According to the model [2,6,7,28], the Gaussian standard deviation σ may yield the values between 0.03 and 0.10 V depending on the value of effective BH if the $I-V$ data for one contact dot are obtained over a wide temperature range. The σ value should be smaller than the above values if the $I-V$ data are obtained for many dots of the same contact metal on the same semiconductor substrate (as in our measurements) or over the whole contact area of one dot as in BEEM measurements at one temperature [17,27–29]. The fact that the small values of σ of 0.005–0.006 V for the $I-V$ and $C-V$ BHs by the Gaussian fits can be ascribed to that the measurements have been made over many dots of the same metal on the same semiconductor substrate at one temperature. As indicated above, the BH appears more uniform at high temperature than that at low temperature, and thus the smaller σ values. Consequently, the BH varies slightly around the mean value on a scale large than the width of the depletion region, or the BH varies laterally on a scale less than or comparable to the width of the depletion region. Likely, the linear relationship between experimental effective BHs and ideality factors in Fig. 7 may be explained by lateral inhomogeneities of the BHs in SDs.

Furthermore, Morgan et al. [29] have given histograms of BEEM BHs on Au/n-Si contacts with different donor densities of the Si substrates; the dots have a diameter of 1.5 mm. In their study, Gaussian least-square to data of the Si substrates have given the values between 0.814 and 0.820 eV, that is, BEEM establishes a laterally homogeneous BH of 0.82 eV, and a Gaussian standard deviation of 8 meV for with $N_D = 1.2 \times 10^{15}\,cm^{-3}$. Considering the margins of experimental errors, these BEEM results for Au/n-Si of Morgan et al. [29] confirm the results of our own Au/n-Si SDs with $N_D = 1.04 \times 10^{15}\,cm^{-3}$ that we have obtained by the Gaussian fits of he experimental Schottky BH distributions obtained from the $C^{-2}-V$ and $I-V$ characteristics and by metal-induced gap states (MIGS) and chemical electronegativity concepts.

4. Conclusion

The homogeneous BH value of approximately 0.834 eV for the Au/n-Si diodes was obtained from the linear relationship between experimental effective BHs and ideality factors which can be explained by lateral inhomogeneities. This value is close to the MIGS line of n-Si/metal contacts for the values of 0.029 eV. In addition, we have shown experimentally that the data on the Au/n-Si contacts become an interesting experimental illustration of the theoretical predictions [16]. The

Gaussian fits of he experimental Schottky BH distributions obtained from the $C^{-2}-V$ and $I-V$ characteristics have yielded a mean BH values of 0.808 and 0.809 eV, respectively. These values are in close agreement with value of about 0.805 eV predicted by metal-induced gap states (MIGS) and chemical electronegativity concepts for Au/*n*-Si SDs.

References

[1] F.E. Jones, C. Hafer, B. Wood, R.G. Danner, M. Lonergan, J. Appl. Phys. 90 (2001) 1001.
[2] Y.P. Song, R.L. Van Meirhaeghe, W.H. Laflere, F. Cardon, Solid-State Electron 29 (1986) 633.
[3] R.T. Tung, Phys. Rev. B 45 (1992) 13509.
[4] R.T. Tung, Mater. Sci. Eng. R 35 (2001) 138.
[5] R.T. Tung, in: L.J. Brilson (Ed.), Contacts to Semiconductors, Noyes Publ., New Jersey, 1993.
[6] J.H. Werner, H.H. Guttler, J. Appl. Phys. 69 (1991) 1522.
[7] S. Chand, J. Kumar, J. Appl. Phys. 82 (1997) 5005.
[8] V.W.L. Chin, M.A. Green, J.W.V. Storey, Solid-State Electron 33 (1990) 299.
[9] J. Ohdomari, K.N. Tu, J. Appl. Phys. 51 (1980) 3735.
[10] A. Olbrich, J. Vancea, F. Kreupl, H. Hoffmann, Appl. Phys. Lett. 70 (1997) 2559.
[11] S. Forment, R.L. Van Meirhaeghe, A.D. Vrieze, K. Strubbe, W.P. Gomes, Semicond. Sci. Technol. 16 (2001) 975.
[12] G.M. Vanalme, R.L. Van Meirhaeghe, F. Cordon, P. Van Daele, Semicond. Sci. Technol. 12 (1997) 907.
[13] J.P. Sullivan, R.T. Tung, M.R. Pinto, W.R. Graham, J. Appl. Phys. 70 (1991) 7403.
[14] T.U. Kampen, W. Mönch, Surf. Sci. 490 (1995) 334.
[15] W. Mönch, Phys. Rev. B 37 (1988) 7129.
[16] R.F. Schmitsdorf, T.U. Kampen, W. Mönch, J. Vac. Sci. Technol. B 15 (1997) 1221.
[17] W. Mönch, Semiconductor Surfaces and Interfaces, 3rd ed., Springer, Berlin, 2001, pp. 389, 421, 485.
[18] W. Mönch, J. Vac. Sci. Technol. B 17 (1999) 1867.
[19] S.M. Sze, Physics of Semiconductor Devices, 2nd Ed., Wiley, New York, 1981, pp. 245.
[20] M. Biber, M. Cakar, A. Turut, J. Mater. Sci. Mater. Electron. 12 (2001) 575.
[21] S.J. Weyers, O. Janzen, W. Mönch, J. Phys.: Condens. Matter 11 (1999) 8489.
[22] E.H. Rhoderick, R.H. Williams, Metal–Semiconductor Contacts, Clarendon, Oxford, 1998.
[23] P. Cova, A. Singh, A. Medina, R.A. Masut, Solid-State Electron. 42 (1998) 477.
[24] V. Saxena, R. Prakash, Polym. Bull. 45 (2000) 267.
[25] C. Nuhoglu, S. Aydogan, A. Turut, Semicond. Sci. Technol. 18 (2003) 646.
[26] K. Akkilic, T. Kilicoglu, A. Turut, Physica B 337 (2003) 393.
[27] S. Zhu, R.L. Van Meirhaeghe, C. Detavernier, F. Cardon, G.P. Ru, X.P. Qu, B.Z. Li, Solid-State Elecron. 44 (2000) 663.
[28] E. Dobrocka, J. Osvald, Appl. Phys. Lett. 65 (1994) 575.
[29] B.A. Morgan, W.G. Bi, K.L. Kavanagh, C.W. Tu, A.A. Talin, R.S. Williams, Y. Segawa, T. Yasui, T. Yasuda Mater. Chem. Phys. 46 (2–3) (1996) 224.